**Annales
Geophysicae**

O$^+$ heating associated with strong wave activity in the high altitude cusp and mantle

R. Slapak[1], H. Nilsson[1], M. Waara[1], M. André[2], G. Stenberg[1], and I. A. Barghouthi[3]

[1]Swedish Institute of Space Physics, Kiruna, Sweden
[2]Swedish Institute of Space Physics, Uppsala, Sweden
[3]Space Research Lab, Department of Physics, Al-Quds University, Jerusalem, Palestine

Abstract. We use the Cluster spacecraft to study three events with intense waves and energetic oxygen ions (O$^+$) in the high altitude cusp and mantle. The ion energies considered are of the order 1000 eV and higher, observed above an altitude of 8 earth radii together with high wave power at the O$^+$ gyrofrequency. We show that heating by waves can explain the observed high perpendicular energy of O$^+$ ions, using a simple gyroresonance model and 25–45% of the observed wave spectral density at the gyrofrequency. This is in contrast to a recently published study where the wave intensity was too low to explain the observed high altitude ion energies. Long lasting cases (>10 min) of high perpendicular-to-parallel temperature ratios are sometimes associated with low wave activity, suggesting that high perpendicular-to-parallel temperature ratio is not a good indicator of local heating. Using multiple spacecraft, we show that the regions of enhanced wave activity are at least one order of magnitude larger than the gyroradius of the heated ions.

Keywords. Space plasma physics (Wave-particle interactions)

1 Introduction

The most direct interaction between the solar wind plasma and Earth's ionosphere is constrained to the magnetospheric cusps, where the open magnetic field lines facilitate a path between the two plasmas. In this region solar wind precipitation yields high ionospheric electron temperatures which leads to strong ionospheric upflow (Nilsson et al., 1996; Ogawa et al., 2003). Strong wave activity is observed, and thus it is the most promising region in which to study wave-particle interaction and its effect on ion outflows and ion escape. Upflowing ionospheric plasma is in general gravitationally bound, and will return as ionospheric downflow unless there is enough energization for the plasma to overcome gravity and reach the magnetosphere (Seki et al., 2002). Plasma in the high-altitude magnetosphere is free of Earth's gravity and heating of oxygen ions (O$^+$) in the cusp serves primarily to put them on trajectories that are more likely to escape downstream rather than being caught up in the closed inner magnetospheric circulation.

Three acceleration mechanisms often considered important for ion escape are centrifugal acceleration, field-aligned potential gradients and wave-particle interactions. Norqvist et al. (1996) studied events of O$^+$ heating in the high-latitude, dayside magnetosphere. The data was obtained from the Freja satellite for altitudes around 1700 km and O$^+$ ions were heated perpendicularly to the background magnetic field to mean energies of about 20 eV, i.e. enough to overcome gravity. The heating was associated with broadband waves. Bouhram et al. (2003b) studied mid-altitude heating events measured by the Interball-2 satellite up to 5 Earth radii (R_E). These observations also indicated that broadband waves are associated with ion heating. In both studies there was sufficient spectral density to explain the heating, using only a few percent of the observed wave spectral density at the O$^+$ gyrofrequency (f_{O^+}). It is not clear which type of waves builds up this broadband spectrum or how much of it is due to waves and how much is due to electrostatic structures. However, it is not likely that all of the wave intensity is effective in the process of ion heating.

A study on the altitude dependence of transversely heated O$^+$ distributions up to 5.5 R_E in the cusps was made by Bouhram et al. (2004) and a saturation of perpendicular heating above 4.5 R_E was reported. This was suggested to be a result of finite perpendicular wavelength effects in the wave-particle interactions. High altitude observations indicate however strong energization of O$^+$ in the high altitude mantle/polar cap region (6–12 R_E). Cluster Ion Spectroscopy

(CIS) measurements show high perpendicular O^+ temperatures and the distribution functions show some enhancement of the perpendicular-to-parallel temperature ratio, $T_r = T_\perp/T_\parallel$ (Arvelius et al., 2005; Nilsson et al., 2006).

In the companion paper by Waara et al. (2011) the wave activity at high altitudes is statistically described. It is shown that mean wave intensities can explain the mean O^+ temperatures between 8 and 15 R_E. In a case study of an enhanced perpendicular heating event at high altitude (12 R_E) made by Waara et al. (2010) the high perpendicular temperature (8000 eV, which is about one order of magnitude higher than the mean temperature at the same altitude) could not be explained with simultaneous wave observations. If the heating is sporadic the chances to observe the heating when it actually takes place may be slim. Ions will retain their energy after heating ceases, and remain heated in the perpendicular direction for some time (the mirror force will gradually transform perpendicular energy to parallel energy for upflowing ions). Therefore high $T_\perp$ and low wave activity should not be seen as a contradiction - even though the high $T_\perp$ associated with the event studied by Waara et al. (2010) could not be explained we do not reject the gyroresonance model, but still consider it as possibly relevant at high altitudes.

We have picked three events with wave intensities significantly higher than mean intensities to investigate if the gyroresonance model is able to explain enhanced perpendicular temperatures (significantly higher than mean temperatures at the corresponding altitudes). This paper together with Waara et al. (2011) complement the statistical study reporting transverse heating of O^+ in the high altitude regions (Nilsson et al., 2006) and the case study performed by Waara et al. (2010).

2 Measurements

For our analysis we use data from instruments onboard the Cluster spacecraft (Escoubet et al., 2001). These four spacecraft are in formation orbiting the Earth and each one carries 11 different instruments, constructed for specific tasks. The ones used in this study are described below.

2.1 Instruments

The Cluster Ion Spectroscopy experiment (CIS) consists of two instruments, a COmposition DIstribution Function (CODIF) analyzer and a Hot Ion Analyzer (HIA). We present results from the CODIF instrument, which has mass resolution and can resolve the major magnetospheric ion species (H^+, He^+, He^{++}, and O^+) by using an ion time-of-flight technique. The CIS experiment provides us with data for the composition and distribution of ions in the plasma. The measured energies range from 15 eV per charge up to 38 keV per charge with a resolution of $\Delta E/E = 0.16$. The angular

resolution is 22.5°. A more detailed description of the CIS instruments can be found in Rème et al. (2001).

The Fluxgate Magnetometer (FGM) provides us with measurements of the magnetic field vector with a sample frequency of 22.4 Hz in the normal mode (Balogh et al., 2001). It consists of two triaxial fluxgate magnetic field sensors which can record three field components, with amplitude resolution of the order $\sim 10^{-4}$ of the background magnetic field. The Electric Field and Wave experiment (EFW) is designed to measure the electric field vector with a sample frequency of 25 Hz in the normal mode (Gustafsson et al., 2001). EFW consists of four probes placed such that they are forming a cross with the spacecraft in the centre. The electric field is deduced by measuring the potential difference between two probes opposing each other, such that two orthogonal field components in the satellite spin plane are recorded. Thus it is a 2-D measurement in the spin plane. This is sufficient for the purpose of this paper, since the electric fields heat the ions perpendicularly to the background magnetic field and the spin axis of the satellite is generally close to parallel to the background magnetic field.

2.2 Data sets

The particle data we are considering is taken from a data set constructed and described by Nilsson et al. (2006). It consists of CODIF data, obtained at high altitudes (5 to 15 R_E) above the polar cap, covering the presence of outflowing O^+, where only beam events lasting longer than one hour were included. The temperatures are mass specific and calculated as moments of the observed particle distributions. The limited energy resolution causes problems when calculating the lowest temperatures (smaller than the kinetic energy of the drift). However, this is not a problem for the strong heating events considered in this study.

The wave data set is constructed such that it covers the same time intervals as the particle data. A typical value of the O^+ gyrofrequency (f_{O^+}) at high altitudes is of the order 10^{-1} Hz and we restrict the data to frequencies ≤ 1 Hz. We go through the data sets manually to find cases of strong wave intensities (clearly stronger than mean wave intensities) where we simultaneously observe enhanced O^+ temperatures. The electric field data (subscripted E) is obtained from the EFW instrument, and the FGM instrument provides us with the corresponding magnetic field data (subscripted B). The magnetic field data is detrended, such that the background magnetic field is ignored.

Power spectral densities are computed using FFT (Fast Fourier Transform) with a record length of 1024 points (corresponding to 41 and 46 s, respectively). We average over three consecutive time records, where each record is shifted 512 points with respect to the previous. From the average spectrograms we get the power spectral densities at the local O^+ gyrofrequency (S_E and S_B, respectively) with a resolution of 20–23 s (512 data points). We will almost exclusively

deal with electric power spectral densities S_E and we will omit the subscript from now on, unless there is a risk for confusion.

In this study we have only used this wave data set as a tool for comparing wave activity associated with O^+ heating events. In the companion paper the statistical properties of the high altitude electric and magnetic fields are presented (Waara et al., 2011).

3 Heating model

The events we are describing in this paper stand out from the surrounding conditions both in terms of higher perpendicular temperatures and increased wave activity. The spacecraft observe these events only for a limited time of a few minutes.

If increased wave activity is mainly a temporal phenomena, the particles flowing out along the field lines will experience the increased wave activity for a similar period of time as the observation time at the spacecraft. If the increased wave activity corresponds to a spatial region, the ions will experience the enhanced wave activity as they drift through the heating region, assuming the heating region is stationary with respect to magnetospheric convection. The latter is known to occur for the region of strong heating associated with the equatorward edge of the cusp at low and mid-altitudes, named the "polar cap heating wall" by Knudsen et al. (1994). Dubouloz et al. (2001) and Bouhram et al. (2003a) described the effect of the "heating wall" on ions spending some time in the heating region and then convecting further into the polar cap where the wave particle interaction is weaker, corresponding to the situation usually described as the polar wind ion outflow. In such a case one can try to estimate the spatial extent of the heating region, and through measurements of the convection calculate the time the particles would have experienced increased wave activity.

The final possibility is that the wave activity is drifting with the plasma. There is then no obvious limit for how long the ions may have experienced the increased wave activity. Ions take considerable time to move along the field line from the ionosphere to the high altitude polar cap/mantle so it is unlikely that wave activity remains strong in a spatially limited region drifting with convection for all that time.

A statistical analysis of the wave activity in the high altitude cusp/mantle shows indeed that wave activity at a given altitude varies by about two orders of magnitude and strong wave activity is typically observed only for a few minutes on each occasion (Waara et al., 2011). Considering these uncertainties in the spatial and temporal extent of the regions of enhanced wave activity, we have developed a simple scheme where we backtrace particles from the observation point down to an apparent start altitude. The rationale for this scheme is to estimate for how long the ions must have experienced the enhanced wave activity in order to explain

the observed perpendicular temperatures, and to see if this is consistent with the simultaneously observed parallel velocity. The latter is important because as long as the heating rate is greater than the adiabatic cooling due to the mirror force we can obtain any perpendicular temperature given enough time. However, if the heating goes on for too long, the mirror force will transfer too much of the energy into the parallel direction, and consequently the parallel velocity may become much higher than what is observed.

3.1 Broadband resonance heating

A model presented in the paper of Chang et al. (1986) considers left-hand polarized waves in a broadband frequency spectrum as a possible mechanism for transverse heating of positively charged ions. This model has turned out to be successful in explaining heating perpendicular to the background magnetic field in the magnetosphere at low and mid-altitudes (Norqvist et al., 1996; Bouhram et al., 2003b), since only a small part of the observed wave spectral density is sufficient in order to explain the heating.

The model is based on the assumption that an ion that travels through a region with broadband waves is in local resonance with some left-hand polarized electromagnetic wave, transverse to the background magnetic field. Considering a gyrotropical distribution the net heating rate for a resonant positively charged ion is

$$\frac{dW_{\text{wave}}}{dt} = S_L \frac{q^2}{2m}, \tag{1}$$

where m is the ion mass, q the ion charge and $S_L = S_L(f_i)$ the power spectral density of the electric field at the ion gyrofrequency, f_i, due to left-hand polarized waves. The net effect is positive since the energy gain for ions in phase is somewhat bigger than the energy loss for ions in antiphase. The net effect of non-resonant waves is approximately zero. As the ion gains energy some of its perpendicular energy is converted into parallel energy due to the mirror force, accelerating the particle along the field line. As the particle moves it will continuously interact with those waves that are in local resonance with it. The total perpendicular heating rate can now be expressed as

$$\frac{dW_\perp}{dt} = \frac{dW_{\text{wave}}}{dt} - \frac{dW_{\text{mir}}}{dt}, \tag{2}$$

where dW_{mir}/dt is the perpendicular adiabatic cooling due to the mirror force, converting perpendicular energy into parallel energy. Assuming a background dipole field and radial field lines (which is roughly true above the polar cap) this term can be written as

$$\frac{dW_{\text{mir}}}{dt} = 3W_\perp \frac{v_\parallel}{r}, \tag{3}$$

where $W_\perp$ is the perpendicular energy of the ion, $v_\parallel$ its parallel velocity and r the geocentric altitude.

3.2 The mean-particle theory

The mean-particle theory (also presented by Chang et al., 1986) gives estimates of both the perpendicular and the parallel temperature (and thus the ratio between them) and a comparison with the observed temperatures is interesting. Below follows a brief description of the theory and the results are discussed in Sect. 5. The theory considers the average rate of resonant heating for an ensemble of particles moving along a dipole field line. The power spectral density is approximated with a power law $S(f) \propto f^{-\alpha}$ with α as a power law fitting parameter, and the gyrofrequency is assumed to decrease with the cube of the geocentric distance, $f_i(r) \propto r^{-3}$. An asymptotic analysis shows that the perpendicular-to-parallel energy ratio approaches $(6\alpha + 2)/9$ and in this limit the total mean energy as a function of altitude becomes

$$W = W_\perp + W_\parallel = \left(3\alpha + \frac{11}{2}\right)^{1/3} m \left[\frac{r D_\perp(r)}{(3\alpha + 1)}\right]^{2/3}, \qquad (4)$$

where the diffusion rate perpendicular to the background magnetic field is defined as $D_\perp(r) = S_L(r) q^2 / 4m^2$ (Retterer et al., 1987). The mean perpendicular and parallel components can be derived from the formulas above (Barghouthi, 1997) and we get

$$W_\perp = \frac{(6\alpha + 2)m}{2^{1/3}} \left[\frac{r D_\perp(r)}{(3\alpha + 1)(6\alpha + 11)}\right]^{2/3}, \qquad (5)$$

$$W_\parallel = \frac{9m}{2^{1/3}} \left[\frac{r D_\perp(r)}{(3\alpha + 1)(6\alpha + 11)}\right]^{2/3}. \qquad (6)$$

These expressions are the estimates of the mean-particle theory derived under the assumption that the electric power spectral density is frequency dependent and does not vary explicitly with altitude. The power spectral density at the oxygen gyrofrequency will vary with altitude because the gyrofrequency varies with altitude. Barghouthi et al. (1998) processed data obtained from the Plasma Wave Instrument (PWI) aboard the DE-1 satellite and found that the average power spectral density is explicitly altitude dependent, as did Waara et al. (2011). However, the case-to-case variability is larger than the average altitude dependence so we will use the observed power spectral densities without assuming any explicit altitude dependence.

3.3 Test-particle calculation

A single-particle calculation code was made, based on Eqs. (1)–(3). Thus we ignore the effects of the polarization electric field and gravitation, which in these cases are negligible compared to the effect of wave-particle interactions and the mirror force. For a suitably small time Δt, the energy changes are

$$\Delta W_\perp = S_L \frac{q^2}{2m} \Delta t - 3W_\perp \frac{v_\parallel}{r} \Delta t, \qquad (7)$$

$$\Delta W_\parallel = 3W_\perp \frac{v_\parallel}{r} \Delta t, \qquad (8)$$

where $S_L = S_L(f_i) \propto r^{3\alpha}$ and the mirror force is described according to motion in a dipole field under the conservation of the magnetic moment. For a time step Δt, the parallel velocity ($v_\parallel$) and the perpendicular energy ($W_\perp$) of the test particle are updated accordingly to the small changes in energy. Using the updated parallel velocity, also the location of the particle is updated ($\Delta r = v_\parallel \Delta t$). The heating rate and the effect of the mirror force are then applied again.

If the model is run in the forward direction this should be done until the test particle reaches the altitude of observation. If the model is run backward it can be run until either the parallel velocity or the perpendicular energy reaches zero, which would correspond to our start altitude.

What would the physical significance of this apparent start altitude be? The ions must have had some parallel velocity and perpendicular energy at the apparent start altitude to which we backtrace it. If most of the heating giving rise to the observed perpendicular energy occurred close to the spacecraft, then the region between our apparent start altitude and the spacecraft shows the altitude extent/time of strong heating. At the apparent start altitude the particles must have had a small perpendicular energy as compared to the observed temperature (at least an order of magnitude lower). The same holds for the parallel velocity. With observed parallel velocities of the order $100\,\mathrm{km\,s^{-1}}$ and perpendicular energies of several keV, this means that the ions should have had parallel velocities below $10\,\mathrm{km\,s^{-1}}$ and perpendicular energies below a few $100\,\mathrm{eV}$ at the apparent start altitudes, which seems feasible. The stronger the perpendicular heating close to the spacecraft is, the higher the parallel velocity at the start of the enhanced heating may have been. Strong perpendicular heating well below the spacecraft will essentially only affect the parallel velocity in the observations, as most of the perpendicular energy gained at low altitude will have been transferred to the parallel direction by the mirror force.

An observation involves an ensemble of particles whose distribution defines a temperature. The test-particle calculation takes only one particle into consideration, and we can only take its kinetic energy into consideration. Therefore we define a typical ion by giving it a perpendicular energy $W_\perp$ equal to the observed perpendicular temperature $T_\perp$.

The calculation is done backwards in time and the input parameters are the observed values for perpendicular temperature $T_\perp$, parallel bulk velocity $v_\parallel$, and geocentric altitude r. The calculation is stopped as $W_\perp$ or $v_\parallel$ is close to zero, and the output corresponds to the values at the apparent start altitude (indexed with 0). The electric power spectral density due to left-hand polarized waves varies with altitude, $S_L(f_i) \propto r^{3\alpha}$. We try different input values of S_L to find $S_{L\,\mathrm{min}}$, which corresponds to the smallest input value needed in order to obtain the observed perpendicular temperature.
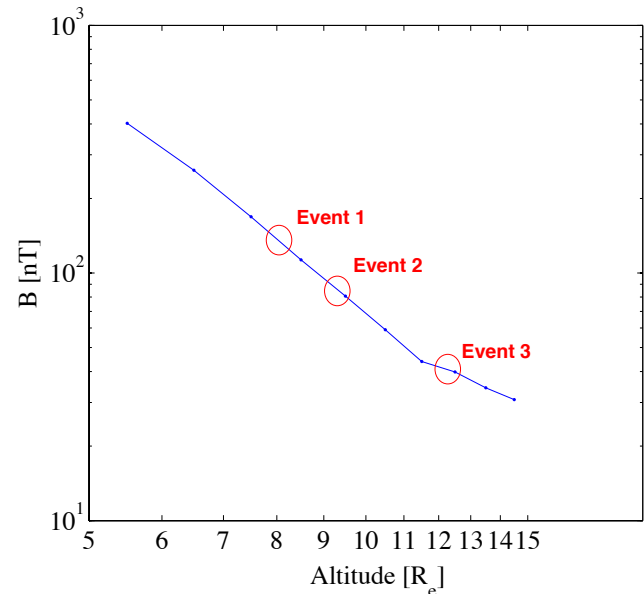
4 Observations

The events studied in this paper were picked from a data set covering the presence of O^+ outflows during the months of January to May in the years 2001, 2002 and 2003, which corresponds to passes of the Cluster spacecraft over the polar caps at high altitudes. For the event studied by Waara et al. (2010), the observed power spectral density was too low in order for the gyroresonance model to explain the high perpendicular temperature (∼8000 eV). This inspired us to create a wave data set (Sect. 2.2) in order to find strong wave activity. We picked cases of high power spectral densities at f_{O^+}, significantly higher than the wave intensities observed in Waara et al. (2010), and where we simultaneously observed enhanced perpendicular O^+ temperatures (of the same order as observed in Waara et al., 2010) in hope of being able to explain them with the gyroresonance model. The data consists of beam events lasting more than one hour. However, the heating events themselves last typically only a few minutes.

The cases have distinct differences. First we consider a case (Event 1) that resembles the general cases at low and mid altitudes. The next case (Event 2) takes place in a more magnetosheath-like region. We close our study with Event 3 that resembles the case studied by Waara et al. (2010). These cases are marked as red circles in Fig. 1, which shows the logarithmic relation between the background magnetic field magnitude and the altitude for our data set. Up to about 11 R_E the background magnetic field falls off as $B \propto r^{-3}$ (dipole). Further up a dipole approximation is not valid anymore since $B \propto r^{-1.75}$. Event 1 and Event 2 clearly take place within the dipole region, whereas Event 3 does not. We take this into consideration in our simulations by proper adjustments of Eqs. (7) and (8) when needed.

4.1 Event 1: 28 May 2003

This heating event (Fig. 2) lasts about 5 min (01:55–02:00 UT) and takes place well inside the magnetosphere at an altitude of around 8.0 R_E (with GSE coordinates (3.1, −3.2, 6.6) R_E), in the Northern Hemisphere over the polar cap. Stable background magnetic fields and small magnetic fluctuations makes it somewhat similar to the heating cases at lower altitudes. The perpendicular temperature reaches a maximum of ∼3000 eV and the parallel ∼1000 eV. Clearly associated to the high temperatures are enhanced electric field power spectral densities. Considered data is measured by spacecraft 4 (SC4). The velocity space distribution function is shown in Fig. 4a, with cross sections through the center of the distribution function shown below (Fig. 4d). The lower plot also shows a Maxwellian (dashed black line) and a kappa distribution (solid black line), both corresponding to the observed perpendicular temperature. Both cross sections seem to be fairly well approximated by Maxwellian distributions.

Fig. 1. The average magnetic field magnitude as a function of altitude (logarithmic scale) for our data sets. The red circles corresponds to the regions where the heating events take place.

Figure 3a shows the power spectral density (up to 1 Hz) during the time interval of heating. It takes the form of an approximate power law distribution $S \propto f^{-\alpha}$ (with $\alpha = 1.1$), for which the power spectral density at f_{O^+} is $S_{f_{O^+}} = 24$ $(mV\,m^{-1})^2\,Hz^{-1}$. The red vertical line in the plot marks $f_{O^+} = 120$ mHz. The green line in the same plot is for a time period close to the heating where the high temperatures as well as wave activity has ceased.

In Sect. 3.3 the test-particle calculation procedure was described, but it will not be a valid approximation unless the heating region is large compared to a typical local ion gyroradius. In Fig. 2c we compare the wave activity from the different spacecraft, with SC4 data corresponding to the blue thick line. Both SC1 (green) and SC4 measure enhanced wave activity (as well as enhanced O^+ temperatures) with similar structures and a time delay of 90 s between the observations. If we assume a heating region structure with a plane front moving with the convecting plasma it would reach SC4 before SC1. This is not the case, so the observed delay between the spacecraft is not consistent with a structure moving with the bulk plasma drift. However, even though there is a time delay between the observations there is a period of time where both spacecraft are in the heating region. An estimate of the heating region extent is thus the distance between the two spacecraft (∼ 0.5 R_E). On the other hand, assuming that the motion of the heating region (v_{hr}) is described by the time delay between SC1 and SC4, the motion of the heating region is ∼ 35 km s^{-1}, and since SC4 observes enhanced wave activity for approximately 240 s this corresponds to a size of 1.3 R_E of the heating region. SC2 is at a similar altitude as

Table 1. Observed O^+ parameters: altitude r, parallel velocity $v_\parallel$, power law fitting parameter α around the local gyrofrequency, electric power spectral density $S_{f_{O+}}$ (given in $(mV\,m^{-1})^2\,Hz^{-1}$), perpendicular temperature $T_\perp$, parallel temperature $T_\parallel$ and perpendicular-to-parallel temperature ratio T_r.

Event	r [R_E]	$v_\parallel$ [km s^{-1}]	α	$S_{f_{O+}}$	$T_\perp$ [eV]	$T_\parallel$ [eV]	T_r
1	8.0	100	1.1	24	3000	1000	3
2	9.3	90	1.1	18	2000	2000	1
3a	12.2	200	1.4	28	7000	5000	1.4
3b	12.2	200	2.1	200	12 000	5000	2.4

Table 2. Calculated parameter values from the backward simulation. r_0 is the geocentric altitude at which the heating starts, t is the heating time, $S_{L\,min}$ and $S_{f_{O+}}$ (given in $(mV\,m^{-1})^2\,Hz^{-1}$) are the input value of the power spectral density due to left-hand polarized electric fields needed to obtain the observed perpendicular temperatures and the observed power spectral density respectively. The ratio $S_r = S_{L\,min}/S_{f_{O+}}$ show how much of the observed power spectral density that needs to be due to left-hand polarized electric waves, in order to obtain the observed perpendicular temperature.

Event	r_0 [R_E]	t [s]	$S_{L\,min}$	$S_{f_{O+}}$	S_r [%]
1	7.1	160	10	24	42
2	8.0	250	5	18	28
3a	9.1	250	26	28	93
3b	10.1	175	53	200	27

the others but does not record any significant wave activity. It is feasible to assume that the size of the heating region is in the range 0.5–1.3 R_E. It can not be smaller and it is not likely to be much larger since no activity is recorded at SC2. A typical O^+ gyroradius in this region is $\sim 0.025\,R_E$, i.e. much smaller than the heating region. For SC3 there is no data available during this event.

We start the test particle calculation at the observation point and trace the particle backwards in time until $T_\perp$ is close to zero. This will give us an estimate of the start altitude and of the spectral density S_L needed. Our input values are $T_\perp = 3000$ eV, $v_\parallel = 100$ km s^{-1}, $r = 8.0\,R_E$ and $\alpha = 1.1$. The input numbers for all events are summarized in Table 1. The minimum power spectral density at f_{O+} due to left-hand polarized electric waves needed to obtain the observed temperature is $S_{L\,min} = 10\,(mV\,m^{-1})^2\,Hz^{-1}$. The observed temperatures can thus be obtained using 42% of the observed power spectral density (Table 2). The heating begins at $r_0 = 7.1\,R_E$ and takes approximately 160 s.
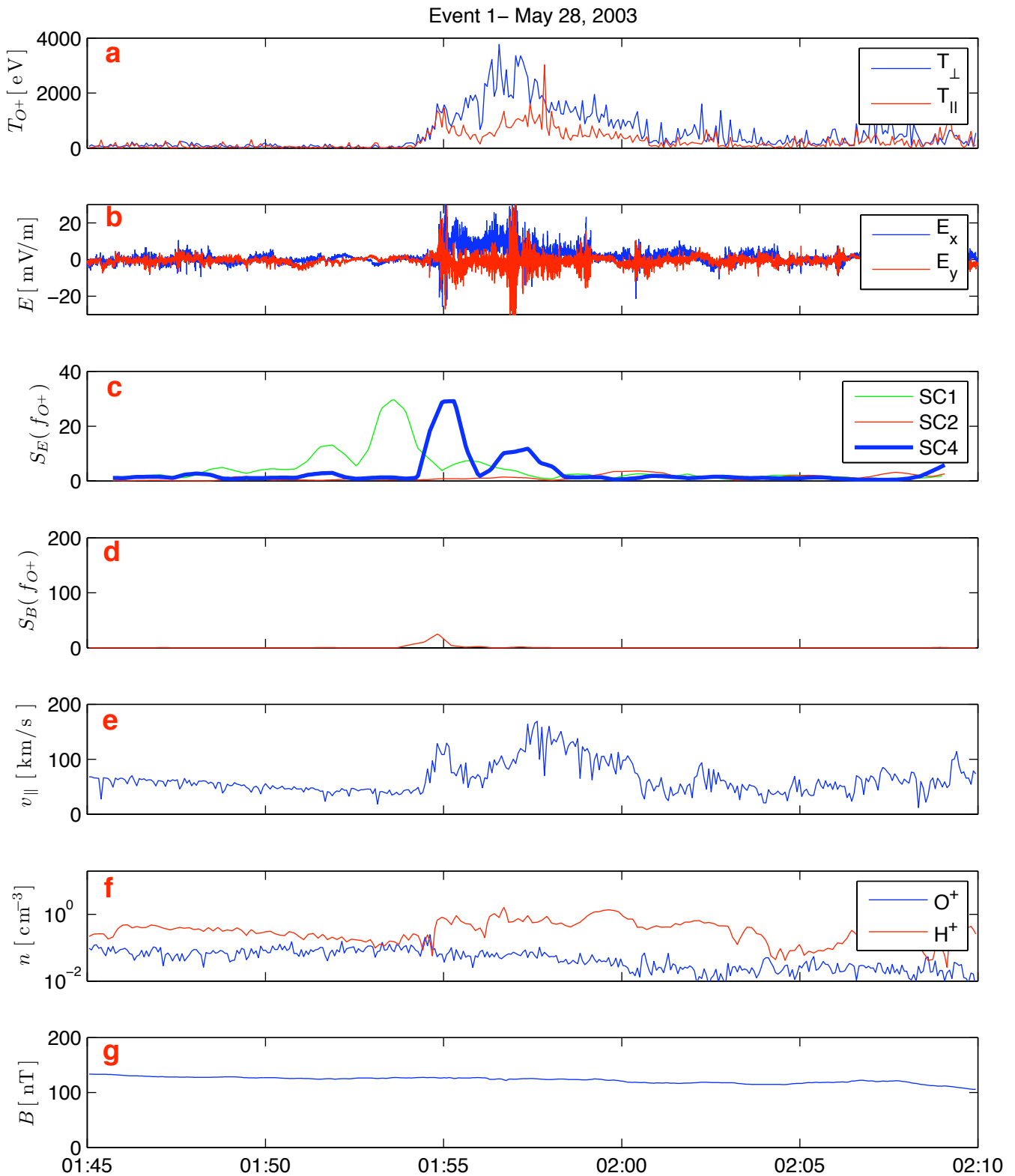
4.2 Event 2: 19 January 2003

This event takes place in a boundary layer between the magnetosheath and the mantle. SC4 is in the magnetosheath before it enters the magnetosphere at around 03:53 UT (Fig. 5), at about 9.3 R_E (GSE coordinates: $(4.4, -0.4, -8.2)\,R_E$),

and measures high ion temperatures and strong wave activity. The temperatures reach roughly 2000 eV. Figure 4b shows the velocity space distribution function. The cross sections through the center of the distribution are shown below (Fig. 4e) and they are both approximate Maxwellian distributions. Particle energies below 2000 eV have been ignored in order to avoid contamination from protons.
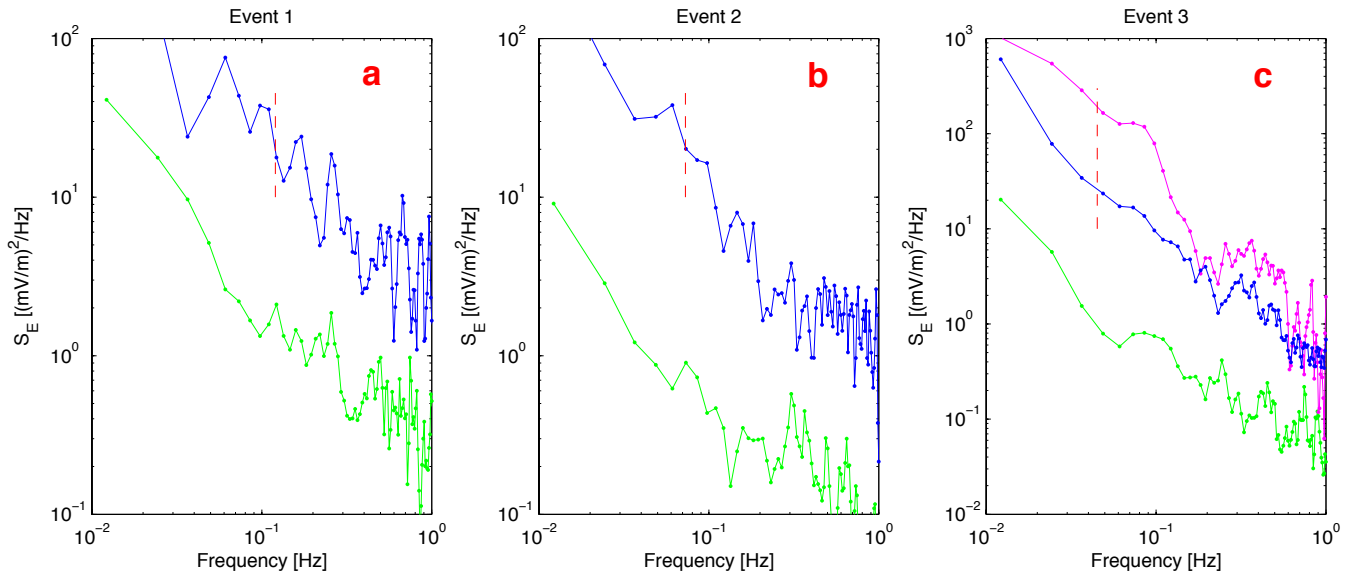
The power density spectrogram (up to 1 Hz) for the heating is shown in in Fig. 3b as a blue curve. The gyrofrequency $f_{O+} = 66$ mHz is marked by a red, dashed line, and it intersects the curve at $S_{f_{O+}} = 18\,(mV\,m^{-1})^2\,Hz^{-1}$. In comparison we have plotted the power spectral density for the time 03:35–03:40 UT (green curve), where the wave activity more or less has ceased. These spectrograms agree well with power law distributions, both with approximately the same power law fitting parameter $\alpha = 1.1$.

We compare the wave intensities measured by the different spacecraft in Fig. 5c. Assuming a plane and field parallel structure extended perpendicular to the convection direction the expected delay between SC2 (red) and SC4 (blue) is small, which is interpreted as if the spacecraft are inside the same structure region approximately at the same time. They are at the same height but separated in the perpendicular direction by a distance of around 1.2 R_E, which then is taken as a lower estimate of the heating region. A typical O^+ gyroradius of 0.06 R_E is much smaller and we can safely use the gyroresonance model. There is a short and strong peak in wave intensity measured by SC3 (black) at a higher altitude, about 0.6 R_E above SC4. The peak corresponds to a passage through the magnetopause and there is no wave activity coupled to the heating region in which we are interested. SC1 (not shown) is further away on the flank ($\sim 1.1\,R_E$) and does not record any enhanced temperatures nor wave intensities.

The input parameters (our observed values) for the test-particle calculation are given in Table 1. The minimum power spectral density at f_{O+} due to left-hand polarized electric waves needed to obtain the observed temperature is $S_{L\,min} = 5\,(mV\,m^{-1})^2\,Hz^{-1}$, corresponding to 28% of the observed power spectral density at f_{O+}. The heating starts at an altitude of 8.0 R_E, with $T_\perp$ and $v_\parallel$ close to zero, and reaches the observed temperatures after 250 s (Table 2).

Fig. 2. SC4 measurements for Event 1 (28 May 2003): Panel **(a)** shows the perpendicular (blue) and the parallel (red) O^+ temperatures, panel **(b)** the electric field for the two components measured in the satellite spin plane, panel **(c)** the power spectral density at f_{O^+} for the electric field given in $(mV\,m^{-1})^2\,Hz^{-1}$ measured by different spacecraft (the blue line corresponds to SC4), panel **(d)** the power spectral density at f_{O^+} for the magnetic field given in $(nT)^2\,Hz^{-1}$, panel **(e)** shows the O^+ parallel velocity, where the outflow is defined to be positive, panel **(f)** the number densities for O^+ (blue) and H^+ (red), and panel **(g)** the magnitude of the background magnetic field.

Fig. 3. Observed power spectral densities for the studied events, which can be approximated with power law distributions. Blue plots: Cover the intervals where we observe strong wave activity for each event. The vertical red lines mark the O^+ gyrofrequency for those regions (120, 66, and 45 mHz respectively). Green plots: For comparison we also plot for regions close to the heatings, where temperatures as well as wave activities are low. Purple plot: This power law distribution covers the $T_\perp$-peak seen around 08:40 UT during Event 3.

4.3 Event 3: 1 May 2003

The last event is presented in (Fig. 6). It is observed at the altitude 12.2 R_E (at the GSE coordinates (0.5, −7.8, −9.4) R_E) and the background magnetic field is between 50 and 60 nT. We divide it into two separate heating cases. Between 08:39–08:46 UT we observe strong wave activity (electric and magnetic) as well as high $T_\perp = 7000$ eV and $T_r = 1.4$. We call this Event 3a. We also note a peak in $T_\perp$ as it for a short period of time around 08:41 UT reaches 12 000 eV and $T_r = 2.4$. Around the same time there is also a peak in the wave activity. We call this Event 3b. Following this (08:46–09:10 UT) we observe high perpendicular temperatures (up to 8000 eV), lower parallel temperatures (up to 2000 eV) and practically no electric and magnetic wave activity, which makes this region similar to the case considered by Waara et al. (2010). Figure 4c shows the velocity space distribution function and below are the cross sections through the center of the distribution (Fig. 4f). Particle energies below 3000 eV have been ignored in order to avoid contamination from protons. One may discern that a torus distribution has begun to form in a part of the distribution, for particles with a parallel velocity of about 200 km s^{-1}. Otherwise, the distribution is quite well approximated by a Maxwellian distribution.

The power spectral densities are plotted in Fig. 3c. During Event 3a (08:39–08:46 UT), the power spectral density (blue curve) at the O^+ gyrofrequency is $S_{f_{O^+}} = 28$ (mV m^{-1})^2 Hz^{-1}. It is in a good agreement to an approximate power law distribution with $\alpha = 1.4$. For Event 3b (purple curve) we observe $S_{f_{O^+}} = 200$ (mV m^{-1})^2 Hz^{-1} and

$\alpha = 2.1$. After 08:50 UT the wave activity has more or less ceased (green curve).
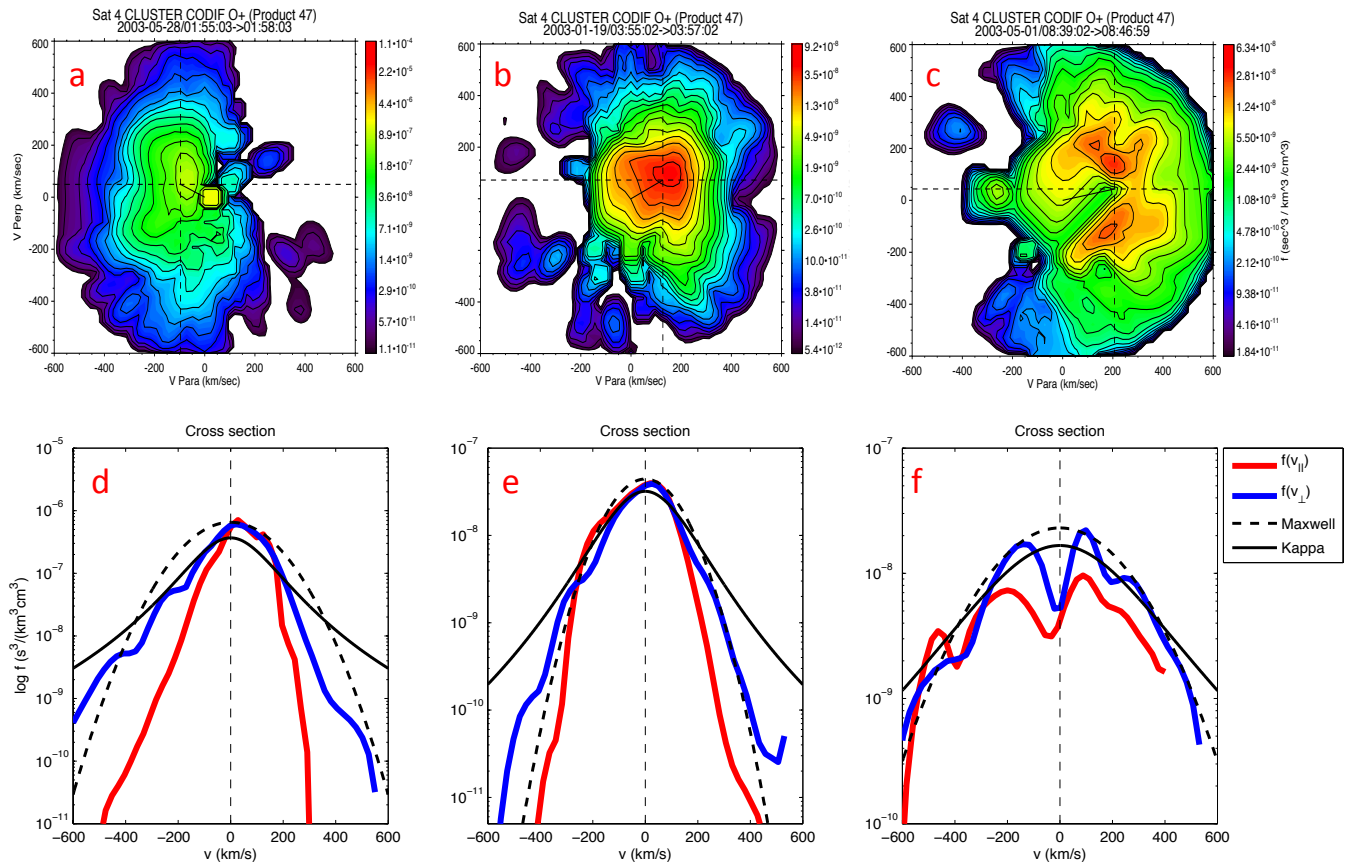
The wave intensities recorded by the spacecraft are shown in Fig. 6c. Comparisons between the different spacecraft assuming a plane and field parallel heating region structure extended perpendicularly to the convection direction yield small delays. SC3 (black) and SC4 (blue) are separated only in height, so it is not possible to get an estimate of the extent of the heating region in the perpendicular direction. SC2 (red) is on the other hand at the same height as SC4 but separated by 1.2 R_E, which gives a lower estimate of the extent of the heating region in the perpendicular direction. This is several times larger than a typical gyroradius at this altitude ($\sim 0.17\ R_E$).

The single-particle calculation results are given in Table 2. For Event 3a a power spectral density of $S_{L\min} = 26$ (mV m^{-1})^2 Hz^{-1} is needed to obtain the observed temperature. This corresponds to 93% of the observed power spectral density at f_{O^+}. The heating starts at the altitude 9.1 R_E, and lasts for 250 s. The results for the intense peak is $S_{L\min} = 53$ (mV m^{-1})^2 Hz^{-1}, $r_0 = 10.1\ R$ and $t = 175$ s. Thus 27% of the observed power spectral density is needed to obtain the observed temperature.

5 Discussion

In Table 2 the calculated electric field power spectral densities $S_{L\min}$ for our events are listed together with the observed values, $S_{f_{O^+}}$. Also listed is $S_r = S_{L\min}/S_{f_{O^+}}$, which shows how much of the observed spectral densities that need to be
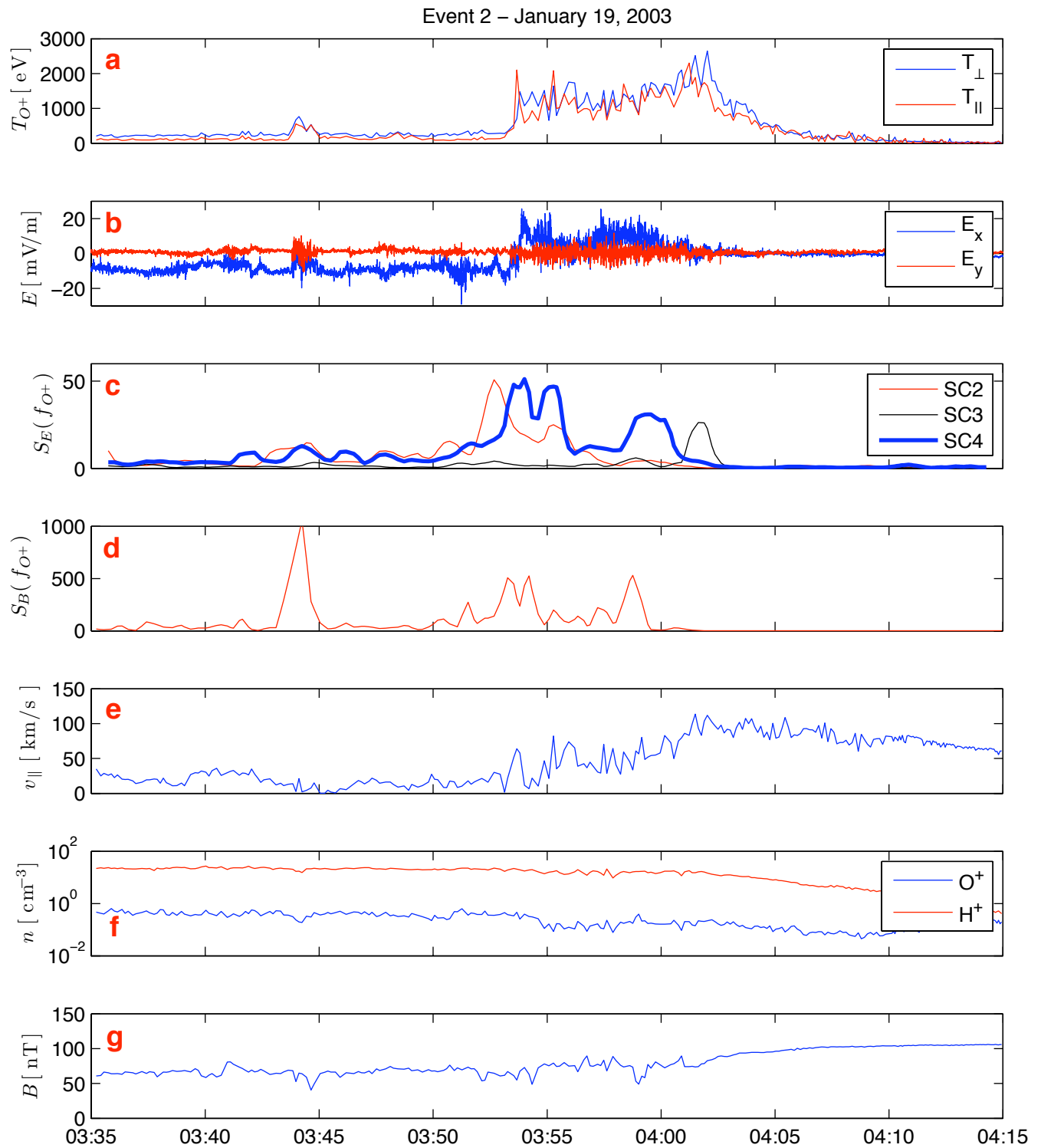
Fig. 4. Velocity space distribution functions of O^+ ions for Event 1 (**a**), Event 2 (**b**) and Event 3 (**c**), respectively. The lower plots (**d**, **e**, **f**) show the corresponding cross sections of the distribution functions in the reference frame of the plasma. Also plotted are Maxwell distributions (dashed black) and Kappa distributions (solid black), corresponding to the observed perpendicular temperature for each event and with $\kappa = 1.5$.

due to left-hand polarized waves in order to obtain the observed perpendicular temperatures. At low and mid altitudes only a few percent is needed. For our cases at high altitudes we need more. Still, for Event 1 and Event 2 the numbers are reasonable (42% and 28%, respectively), whereas for Event 3a 93% is required. This is unrealistic since it requires that practically all observed wave activity is due to left-hand polarized waves. The order of magnitude is still reasonable. Considering the large variability of the electric field wave intensity it is not surprising if we do not get perfect agreement for all cases. The sharp peak (12 000 eV) can be explained if we focus on the wave activity peak in its neighbourhood, since 27% is needed (Event 3b). It seems that we in general need left-hand polarized wave activity with power spectral densities of the order $S_L \sim 10 \ (\mathrm{mV\,m^{-1}})^2 \, \mathrm{Hz^{-1}}$ to be able to explain high perpendicular temperatures.
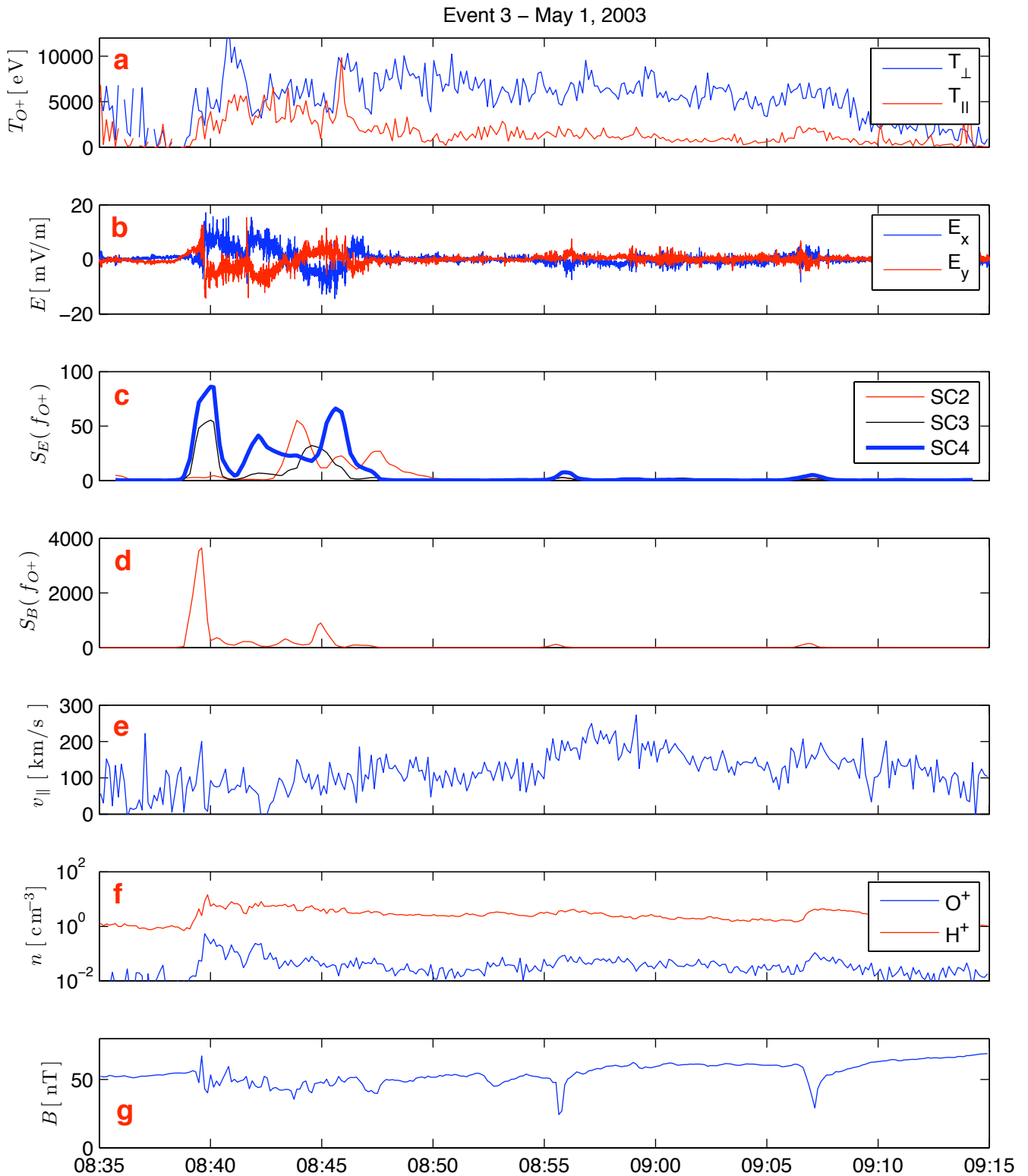
The gyroresonance model is not feasible unless the considered heating region is large compared to a typical local O^+ gyroradius. For all events the estimated perpendicular extent of the heating region is indeed large compared to the O^+ gyroradius. We have analyzed the expected delays be-

tween the spacecraft assuming a heating structure drifting along with the plasma and extended perpendicularly to the convection direction. In Event 1 the analysis also shows that the observed delay between the spacecraft is not consistent with a heating structure moving with the plasma bulk drift. For Event 2 and 3 the delays are small and we cannot get a reliable estimate of the motion of the heating regions.

In a previous study by Bouhram et al. (2004) it was shown that cusp related heating of outflowing ions appeared to saturate above $4.5\,R_E$. A finite wavelength effect, where the ion gyroradius becomes larger than the perpendicular wavelength of the waves, was suggested as a mechanism behind the saturation. Barghouthi (2008) showed that finite wavelength effects lead to saturation of heating and torus shaped velocity space distributions. In Event 3, indeed a torus shaped velocity distribution is starting to form (Fig. 4a). However, the high temperatures and effective heating that we observe at high altitudes indicate that there is no saturation of the heating. The latter is consistent with the large size of the heating region compared to the local gyroradius. If the ion leaves the field of one wave it will encounter the field of

Fig. 5. SC4 measurements for Event 2 (19 January 2003): Panel **(a)** shows the perpendicular (blue) and the parallel (red) O^+ temperatures, panel **(b)** the electric field for the two components measured in the satellite spin plane, panel **(c)** the power spectral density at f_{O^+} for the electric field given in $(mV\,m^{-1})^2\,Hz^{-1}$ measured by different spacecraft (the blue line corresponds to SC4), panel **(d)** the power spectral density at f_{O^+} for the magnetic field given in $(nT)^2\,Hz^{-1}$, panel **(e)** the O^+ parallel velocity, where the outflow direction is defined to be positive, panel **(f)** the number densities for O^+ (blue) and H^+ (red), and panel **(g)** the magnitude of the background magnetic field.

Fig. 6. SC4 measurements for Event 3 (1 May 2003): Panel **(a)** shows the perpendicular (blue) and the parallel (red) O^+ temperatures, panel **(b)** the electric field for the two components measured in the satellite spin plane, panel **(c)** the power spectral density at f_{O^+} for the electric field given in $(mV\,m^{-1})^2\,Hz^{-1}$ measured by different spacecraft (the blue line corresponds to SC4), panel **(d)** the power spectral density at f_{O^+} for the magnetic field given in $(nT)^2\,Hz^{-1}$, panel **(e)** shows the O^+ parallel velocity, where the outflow direction is defined to be positive, panel **(f)** the number densities for O^+ (blue) and H^+ (red), and panel **(g)** the magnitude of the background magnetic field.

Table 3. Mean-particle theory results: perpendicular energy $W_\perp$, parallel energy $W_\parallel$ and perpendicular-to-parallel energy ratio W_r.

Event	$W_\perp$ [eV]	$W_\parallel$ [eV]	W_r
1	1770	1850	0.96
2	1230	1290	0.96
3a	4830	4180	1.16
3b	7020	4330	1.62

another. This may affect the coherence time, but not lead to saturation.

We based our simple test-particle calculation on Eqs. (1)–(3). This description turns out to be useful to describe the limited (in time and space) bursts of O^+ heating that we observe. It gives us an estimate of the altitude extent below the spacecraft where strong heating seems to take place. It is interesting to see if the observed temperature ratios can be reproduced for the spectral densities of our observations. This can be done by comparing to the mean-particle theory, which is briefly described in Sect. 3.1. Equations (5)–(6) are asymptotic values, obtained considering a frequency dependent power spectral density. Into these equations we put our observed values and $S_L = S_{L\min}$. The ion energies predicted by the theory ($W_\perp$, $W_\parallel$ and W_r) are presented in Table 3. These calculated values are compared to observed temperatures in Table 1 ($T_\perp$ and T_r) and we note that the mean-particle theory results do not agree very well with observations. The theory generally gives too small values (with the exception of the parallel component in Event 1 where it is too large). When the perpendicular-to-parallel ratios are compared we note that they are equal for Event 2, but differ for the others.

Heating events with $T_r > 2$ at high altitudes have been studied before (Waara et al., 2010), as well as cases with $T_r \approx 1$ (Nilsson et al., 2004). In Event 3 we observe both types: $T_r \approx 1$ during strong wave activity followed by a longer sequence (25 min) of enhanced T_r and $T_\perp$ when the wave activity has ceased. If heating is sporadic, one should expect to sometimes find high ion temperatures and simultaneously no or low wave activity, since the particles after heating stay heated in the perpendicular direction some time after their interaction with electromagnetic waves. Sporadic heating is however not a plausible explanation for long sequences of enhanced $T_\perp$ and low $T_\parallel$. For this we suggest a so called velocity-filter effect, where particles with approximately the same parallel velocities are seen in the same place at a given time after the heating. This concept is illustrated and explained in Fig. 1 in Nilsson et al. (2004), considering a finite heating-source region through which particles convect. The fast-moving particles will reach a certain altitude sooner than particles that move slower. The slower particles will of course eventually reach the same altitude, but at that time they will have convected further away. A spacecraft passing above the heating region will therefore continuously encounter narrow parallel velocity distributions, and consequently low parallel temperatures.

We observe increased magnetic wave activity during Event 2 and 3. According to Waara et al. (2011) the observed electric and magnetic field fluctuations are consistent with Alfvén waves, so a relation between electric and magnetic fluctuations is expected. Most studies of the effect of wave-particle interactions on ion outflows (e.g. Chang et al., 1986; Retterer et al., 1987; André et al., 1990; Norqvist et al., 1996; Bouhram et al., 2003a; Barghouthi, 2008), consider only the electric field of the waves to be responsible for transverse ion heating. Wang et al. (2006) and Lu and Li (2007) take the magnetic field of the wave into consideration in their theory of transverse ion heating, but it is done under conditions which are not fulfilled in the region of our interest. May strong magnetic fluctuations affect ion heating in the high altitude magnetosphere? In the magnetosheath-like regions the magnetic field fluctuations can be as strong as 10% of the background field strength. Perhaps the invariance of the magnetic moment does not hold under such conditions. A future statistical study will present a more quantitative correlation between electric and magnetic field wave activity and ion heating.

6 Conclusions

When high altitude O^+ heating events associated with strong wave activity are considered it is possible to explain enhanced perpendicular temperatures, using a gyrofrequency model based on the same theory (Chang et al., 1986) that have been successful in explaining the enhanced perpendicular temperatures at low and mid altitudes (Norqvist et al., 1996; Bouhram et al., 2003b). Using 25–45% of the observed wave activity we can explain the enhanced perpendicular temperature in all but one of the studied cases.

Bouhram et al. (2004) reported saturation of the perpendicular heating above $\sim 4.5\,R_E$ in the cusps and suggested that it was due to finite perpendicular wavelength effects, where the heating is limited when the ion gyroradius exceeds the perpendicular wavelength of the wave. Barghouthi (2008) also discussed the effect of finite wavelength and showed that it saturates heating. However, we observe effective heating and conclude that we do not see any effects of finite wavelengths. One possible reason is larger perpendicular wavelengths in the high altitude range as compared to the altitude range studied by Bouhram et al. (2004). Another possibility is the large perpendicular extent of the heating regions, which are at least about an order of magnitude larger than the local ion gyroradius, which allows the ions to continuously interact with different wave fields.

Observations indicate that enhanced wave activity is limited in time and space. Consequently, strong ion heating is then also limited in time and space. Our calculations

indicate that high-altitude O^+ ions with high temperatures mainly have been heated within a few R_E from where they are observed. This is consistent with the mean-particle theory of Chang et al. (1986) and Retterer et al. (1987) (briefly described in Sect. 3.2) where it was noted that for significant heating the initial boundary conditions are not important, most of the effective heating occur in the vicinity of the spacecraft.

The perpendicular-to-parallel temperature ratio, T_r, is often close to one, but it may also be well above 2 even during times of no significant wave activity. Enhanced perpendicular-to-parallel temperature ratio, T_r, is usually considered as a sign of local heating. At high altitudes relatively low wave activity sometimes appear to be associated with these types of events, which is quite the opposite from what is expected. We clearly see this in Event 3 around 08:46–09:10 UT with high $T_\perp$ and strongly enhanced T_r and practically no wave activity, similar to the case presented by Waara et al. (2010). We suggest that this results from a velocity filter effect when observations are made close to but outside a heating region. Thus, high perpendicular-to-parallel temperature ratio is not a good indicator of local heating in regions at high altitudes.

References

André, M., Crew, G. B., Peterson, W. K., Persoon, A. M., and Pollock, C. J.: Ion heating by broadband low-frequency waves in the cusp/cleft, J. Geophys. Res., 95, 20809–20823, doi:10.1029/JA095iA12p20809, 1990.

Arvelius, S., Yamauchi, M., Nilsson, H., Lundin, R., Hobara, Y., Rème, H., Bavassano-Cattaneo, M. B., Paschmann, G., Korth, A., Kistler, L. M., and Parks, G. K.: Statistics of high-altitude and high-latitude O^+ ion outflows observed by Cluster/CIS, Ann. Geophys., 23, 1909–1916, doi:10.5194/angeo-23-1909-2005, 2005.

Balogh, A., Carr, C. M., Acuña, M. H., Dunlop, M. W., Beek, T. J., Brown, P., Fornacon, K.-H., Georgescu, E., Glassmeier, K.-H., Harris, J., Musmann, G., Oddy, T., and Schwingenschuh, K.: The Cluster Magnetic Field Investigation: overview of in-flight performance and initial results, Ann. Geophys., 19, 1207–1217, doi:10.5194/angeo-19-1207-2001, 2001.

Barghouthi, I. A.: Effects of wave-particle interactions on H^+ and O^+ outflow at high latitude: A comparative study, J. Geophys. Res., 102, 22065–22076, doi:10.1029/96JA03293, 1997.

Barghouthi, I. A.: A Monte Carlo study for ion outflows at high altitude and high latitude: Barghouthi model, J. Geophys. Res. (Space Physics), 113, 8209, doi:10.1029/2008JA013274, 2008.

Barghouthi, I. A., Barakat, A. R., and Persoon, A. M.: The Effects of Altitude-Dependent Wave Particle Interactions on the Polar Wind Plasma, Astrophysics and Space Science, 259, 117–140, doi:10.1023/A:1001569207346, 1998.

Bouhram, M., Malingre, M., Jasperse, J. R., and Dubouloz, N.: Modeling transverse heating and outflow of ionospheric ions from the dayside cusp/cleft. 1 A parametric study, Ann. Geophys., 21, 1753–1771, doi:10.5194/angeo-21-1753-2003, 2003a.

Bouhram, M., Malingre, M., Jasperse, J. R., Dubouloz, N., and Sauvaud, J.-A.: Modeling transverse heating and outflow of ionospheric ions from the dayside cusp/cleft. 2 Applications, Ann. Geophys., 21, 1773–1791, doi:10.5194/angeo-21-1773-2003, 2003b.

Bouhram, M., Klecker, B., Miyake, W., Rème, H., Sauvaud, J.-A., Malingre, M., Kistler, L., and Blăgău, A.: On the altitude dependence of transversely heated O^+ distributions in the cusp/cleft, Ann. Geophys., 22, 1787–1798, doi:10.5194/angeo-22-1787-2004, 2004.

Chang, T., Crew, G. B., Hershkowitz, N., Jasperse, J. R., Retterer, J. M., and Winningham, J. D.: Transverse acceleration of oxygen ions by electromagnetic ion cyclotron resonance with broad band left-hand polarized waves, Geophys. Res. Lett., 13, 636–639, doi:10.1029/GL013i007p00636, 1986.

Dubouloz, N., Bouhram, M., Senior, C., Delcourt, D., Malingre, M., and Sauvaud, J.-A.: Spatial structure of the cusp/cleft ion fountain: A case study using a magnetic conjugacy between Interball AP and a pair of SuperDARN radars, J. Geophys. Res., 106, 261–274, 2001.

Escoubet, C. P., Fehringer, M., and Goldstein, M.: Introduction The Cluster mission, Ann. Geophys., 19, 1197–1200, doi:10.5194/angeo-19-1197-2001, 2001.

Gustafsson, G., André, M., Carozzi, T., Eriksson, A. I., Fälthammar, C.-G., Grard, R., Holmgren, G., Holtet, J. A., Ivchenko, N., Karlsson, T., Khotyaintsev, Y., Klimov, S., Laakso, H., Lindqvist, P.-A., Lybekk, B., Marklund, G., Mozer, F., Mursula, K., Pedersen, A., Popielawska, B., Savin, S., Stasiewicz, K., Tanskanen, P., Vaivads, A., and Wahlund, J.-E.: First results of electric field and density observations by Cluster EFW based on initial months of operation, Ann. Geophys., 19, 1219–1240, doi:10.5194/angeo-19-1219-2001, 2001.

Knudsen, D. J., Whalen, B., Abe, T., and Yau, A.: Temporal evolution and spatial dispersion of ion conics: Evidence for a polar cap heating wall, in: Solar System Plasmas in Space and Time, Geophysical Monograph series, edited by: Burch, J. L. and Waite Jr., J. H., vol. 84, pp. 163–169, AGU (American Geophysical Union), 1994.

Lu, Q. and Li, X.: Heating of ions by low-frequency Alfven waves, Physics of Plasmas, 14, 042303, doi:10.1063/1.2715569, 2007.

Nilsson, H., Yamauchi, M., Eliasson, L., Norberg, O., and Clemmons, J.: The ionospheric signature of the cusp as seen by incoherent scatter radar, J. Geophys. Res., 101, 10947–10963, 1996.

Nilsson, H., Joko, S., Lundin, R., Rème, H., Sauvaud, J.-A., Dandouras, I., Balogh, A., Carr, C., Kistler, L. M., Klecker, B., Carlson, C. W., Bavassano-Cattaneo, M. B., and Korth, A.: The structure of high altitude O^+ energization and outflow: a case study, Ann. Geophys., 22, 2497–2506, doi:10.5194/angeo-22-2497-2004, 2004.

Nilsson, H., Waara, M., Arvelius, S., Marghitu, O., Bouhram, M., Hobara, Y., Yamauchi, M., Lundin, R., Rème, H., Sauvaud, J.-

A., Dandouras, I., Balogh, A., Kistler, L. M., Klecker, B., Carlson, C. W., Bavassano-Cattaneo, M. B., and Korth, A.: Characteristics of high altitude oxygen ion energization and outflow as observed by Cluster: a statistical study, Ann. Geophys., 24, 1099–1112, doi:10.5194/angeo-24-1099-2006, 2006.

Norqvist, P., André, M., Eliasson, L., Eriksson, A. I., Blomberg, L., Lühr, H., and Clemmons, J. H.: Ion cyclotron heating in the dayside magnetosphere, J. Geophys. Res., 101, 13179–13194, doi:10.1029/95JA03596, 1996.

Ogawa, Y., Fujii, R., Buchert, S. C., Nozawa, S., and Ohtani, S.: Simultaneous EISCAT Svalbard radar and DMSP observations of ion upflow in the dayside polar ionosphere, J. Geophys. Res., 108, 1101, doi:10.1029/2002JA009590, 2003.

Rème, H., Aoustin, C., Bosqued, J. M., Dandouras, I., Lavraud, B., Sauvaud, J. A., Barthe, A., Bouyssou, J., Camus, Th., Coeur-Joly, O., Cros, A., Cuvilo, J., Ducay, F., Garbarowitz, Y., Medale, J. L., Penou, E., Perrier, H., Romefort, D., Rouzaud, J., Vallat, C., Alcaydé, D., Jacquey, C., Mazelle, C., d'Uston, C., Möbius, E., Kistler, L. M., Crocker, K., Granoff, M., Mouikis, C., Popecki, M., Vosbury, M., Klecker, B., Hovestadt, D., Kucharek, H., Kuenneth, E., Paschmann, G., Scholer, M., Sckopke, N., Seidenschwang, E., Carlson, C. W., Curtis, D. W., Ingraham, C., Lin, R. P., McFadden, J. P., Parks, G. K., Phan, T., Formisano, V., Amata, E., Bavassano-Cattaneo, M. B., Baldetti, P., Bruno, R., Chionchio, G., Di Lellis, A., Marcucci, M. F., Pallocchia, G., Korth, A., Daly, P. W., Graeve, B., Rosenbauer, H., Vasyliunas, V., McCarthy, M., Wilber, M., Eliasson, L., Lundin, R., Olsen, S., Shelley, E. G., Fuselier, S., Ghielmetti, A. G., Lennartsson, W., Escoubet, C. P., Balsiger, H., Friedel, R., Cao, J.-B., Kovrazhkin, R. A., Papamastorakis, I., Pellat, R., Scudder, J., and Sonnerup, B.: First multispacecraft ion measurements in and near the Earth's magnetosphere with the identical Cluster ion spectrometry (CIS) experiment, Ann. Geophys., 19, 1303–1354, doi:10.5194/angeo-19-1303-2001, 2001.

Retterer, J. M., Chang, T., Crew, G. B., Jasperse, J. R., and Winningham, J. D.: Monte Carlo modeling of ionospheric oxygen acceleration by cyclotron resonance with broad-band electromagnetic turbulence, Phys. Rev. Lett., 59, 148–151, doi:10.1103/PhysRevLett.59.148, 1987.

Seki, K., Elphic, R. C., Thomsen, M. F., Bonnell, J., McFadden, J. P., Lund, E. J., Hirahara, M., Terasawa, T., and Mukai, T.: A new perspective on plasma supply mechanisms to the magnetotail from a statistical comparison of dayside mirroring O^+ at low altitudes with lobe/mantle beams, J. Geophys. Res. (Space Physics), 107, 1047, doi:10.1029/2001JA900122, 2002.

Waara, M., Nilsson, H., Stenberg, G., André, M., Gunell, H., and Rème, H.: Oxygen ion energization observed at high altitudes, Ann. Geophys., 28, 907–916, doi:10.5194/angeo-28-907-2010, 2010.

Waara, M., Slapak, R., Nilsson, H., Stenberg, G., André, M., and Barghouthi, I. A.: Statistical evidence for O^+ energization and outflow caused by wave-particle interaction in the high altitude cusp and mantle, Ann. Geophys., 29, 945–954, doi:10.5194/angeo-29-945-2011, 2011.

Wang, C. B., Wu, C. S., and Yoon, P. H.: Heating of Ions by Alfvén Waves via Nonresonant Interactions, Phys. Rev. Lett., 96, 125001, doi:10.1103/PhysRevLett.96.125001, 2006.